ARMY RESEARCH LABORATORY

Structural Changes in Lipid Vesicles Generated by the Shock Blast Waves: Coarse-Grained Molecular Dynamics Simulation

by Yelena R. Sliozberg

ARL-CR-722 **November 2013**

NOTICES

Disclaimers

The findings in this report are not to be construed as an official Department of the Army position unless so designated by other authorized documents.

Citation of manufacturer's or trade names does not constitute an official endorsement or approval of the use thereof.

Destroy this report when it is no longer needed. Do not return it to the originator.

Army Research Laboratory
Aberdeen Proving Ground, MD 21005

ARL-CR-722 **November 2013**

Structural Changes in Lipid Vesicles Generated by the Shock Blast Waves: Coarse-Grained Molecular Dynamics Simulation

Yelena R. Sliozberg
Bowhead Science & Technology, LLC

REPORT DOCUMENTATION PAGE

Form Approved
OMB No. 0704-0188

1. REPORT DATE *(DD-MM-YYYY)*	2. REPORT TYPE	3. DATES COVERED (From - To)
November 2013	Final	1 September–30 September 2013

4. TITLE AND SUBTITLE
Structural Changes in Lipid Vesicles Generated by the Shock Blast Waves: Coarse-Grained Molecular Dynamics Simulation

5a. CONTRACT NUMBER
W911QX-09-C-0057

5b. GRANT NUMBER

5c. PROGRAM ELEMENT NUMBER

6. AUTHOR(S)
Yelena R. Sliozberg*

5d. PROJECT NUMBER

5e. TASK NUMBER

5f. WORK UNIT NUMBER

7. PERFORMING ORGANIZATION NAME(S) AND ADDRESS(ES)
U.S. Army Research Laboratory
ATTN: RDRL-WMM-G
Aberdeen Proving Ground, MD 21005

8. PERFORMING ORGANIZATION REPORT NUMBER
ARL-CR-722

9. SPONSORING/MONITORING AGENCY NAME(S) AND ADDRESS(ES)

10. SPONSOR/MONITOR'S ACRONYM(S)

11. SPONSOR/MONITOR'S REPORT NUMBER(S)

12. DISTRIBUTION/AVAILABILITY STATEMENT
Approved for public release; distribution unlimited.

13. SUPPLEMENTARY NOTES
*Bowhead Science & Technology, LLC, 103 Bata Blvd., Suite K, Belcamp, MD 21017

14. ABSTRACT
Traumatic Brain Injury is a major health issue that is hard to diagnose because it often happens without external injuries. While it is well known that exposure of biological cells to shock waves causes damage to cell membranes, it is currently unknown how blast waves generated by an explosion cause the cellular structural injury. It is still unclear by which mechanisms damage is caused, and how it depends on physical parameters such as shock-wave velocity, shock-pulse duration, or shock-pulse shape. Used in this computational study is a coarse-grained model of the lipid vesicle as a simplified model of a cell membrane to elucidate the general principles of the cellular damage induced by blast waves. The results show that the cellular membrane permeability is altered even for a relatively mild blast wave (the Mach number M is less than 1.5) in the negative pressure phase. The simulation findings suggest that the small negative pressure approximately -5 psi may lead to the cellular damage by changing the ion influx. The faster-moving shock waves ($M \approx 1.9$) that have higher overpressure peaks cause the cellular damage in the positive pressure phase if peak overpressure is greater than 60 psi.

15. SUBJECT TERMS
TBI, liposome, cellular membrane, simulation, computation

16. SECURITY CLASSIFICATION OF:			17. LIMITATION OF ABSTRACT	18. NUMBER OF PAGES	19a. NAME OF RESPONSIBLE PERSON
a. REPORT	b. ABSTRACT	c. THIS PAGE			Wendy Winner/Dave Weeks
Unclassified	Unclassified	Unclassified	UU	24	19b. TELEPHONE NUMBER (*Include area code*) 410-306-0700

Standard Form 298 (Rev. 8/98)
Prescribed by ANSI Std. Z39.18

Contents

List of Figures

List of Tables

1. Introduction

Traumatic Brain Injury (TBI) is a major health issue that leads to a range of neurological and psychological impairments. In recent operations, hundreds of thousands of U.S. military personnel sustained a mild form of TBI, often after exposure to an explosive blast. Mild TBI is hard to diagnose because it often happens without external injuries, and consequently mild TBI may not be identified until the service member returns home (*1*).

The blast shock wave of primary TBI is a transient supersonic pressure wave with a rapid, less than 1-ms increase in pressure (compression), density, and temperature, which corresponds to the peak overpressure in figure 1, followed by a nonlinear, microsecond phase of low pressure or tension. Such pressure/temperature (*p* versus *t*) curves can be mathematically described by the so-called Friedlander waveform (figure 1). The integration of this curve gives the positive impulse per unit area *I*, which is a useful measure for positive overpressure duration (*2*, *3*).

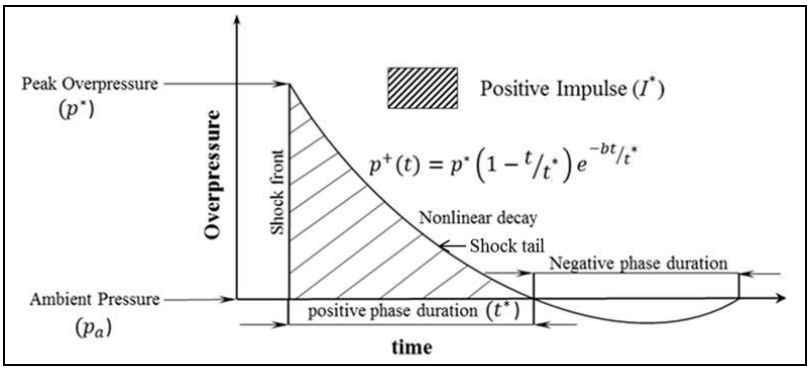

Figure 1. Mathematical representation of planar Friedlander waveform (*3*).

In the majority of TBI cases the peak pressure is low. Even exposure to blasts of 10-atm peak pressure for a few milliseconds can result in death for unprotected people (*4*). The mechanisms initiating TBI as a direct result of the shock wave generated by an explosion remain obscure. Although dynamic compression, tension, and shear stress have all been proposed to explain primary TBI, the precise mechanism of how this damage arises is not fully understood (*5*).

While it is well known that exposure of biological cells to shock waves causes damage to the cell membrane, it is currently unknown how cellular structural damage from realistic blast impact affects cellular function at varied time scales prior to and subsequent to brain traumas. It is still unclear by which mechanisms damage is caused and how it depends on physical parameters such as shock-wave velocity, shock-pulse duration, or shock-pulse shape.

Experimentally, it is very difficult to observe the dynamics of membrane rupture due to small time scales and length scales of the event. Since a typical cell membrane is only several nanometers thick, while the pressure front of a shock wave travels at supersonic speeds (for example, the speed of sound in water is 1497 m/s), the time scale during which a shock wave interacts with a cell membrane is on the order of picoseconds (*2*). As a consequence, it may prove particularly helpful to elucidate the microscopic structural details and dynamics with computer simulations.

Cell membranes are mainly composed of phospholipids, each made of a hydrophilic segment ("head") covalently bonded to a hydrophobic segment ("tail"). The phospholipids form a bilayer stabilized by hydrophobic and hydrophilic interactions. However, simulation of a realistic cell membrane is a challenging task due to the structural complexity of cell membranes. Real brain cell membranes are inhomogeneous structures that include multiple lipids, cholesterol, and numerous proteins. The purpose of this study is not to simulate cell membranes in realistic detail but to focus on a simple model of the major constituent of a cell membrane, the phospholipid bilayer. In this work, we studied the mechanism of shock-wave-induced damage to phospholipid vesicles (liposomes) as the simplified generic model for the cell membranes. Vesicles or liposomes are composed of phospholipids that encapsulate a core region of water inside a hydrophobic membrane. Simulation studies of vesicles have some clear advantages over those of planar membranes: the absence of a periodicity effect, the use of curvature as an additional parameter, and the closer correspondence to experimental studies performed with vesicular systems (*6*).

The standard technique to numerically simulate phospholipid bilayers is molecular dynamics (MD). However, the complexity of the atomistic force fields limits them to membrane patches and vesicles some tens of nanometers in extent for times of tens of microseconds or less. It is questionable whether such small systems can quantitatively reproduce real damage processes for several reasons, including artificial stabilization of the membrane patch due to correlation effects, absence of membrane defects, and curvature, where membrane rupture likely originates from a less-than ideal flat surface. The short simulation time of these models due to a small simulation box makes it impossible to study the time evolution of the shocked membranes where the shock front can travel for a long period of time (*2*).

Various coarse-grained (CG) simulation techniques, including inverse Monte Carlo schemes, force-matching approaches, and calibrated techniques based on thermodynamic data, have been developed for phospholipid membranes that allow them to reach length and time scales inaccessible to atomistic MD by grouping atoms into particles, thereby reducing the number of particles, and fast dynamics make simulations two to three orders of magnitude more efficient than the fully atomistic simulation. Advantages of these approaches include a relatively high level of accuracy and a closer resemblance to atomistic simulations (*6*).

Dissipative Particle Dynamics (DPD) (*7–10*) is a unique CG technique for complex fluids that allows structural and dynamic relaxation to occur 10^4 times faster than a fully atomistic simulation (*10*). DPD captures the mass and momentum conservation that are responsible for the correct hydrodynamic behavior and allows us to simulate the kinetics of the liposome system. On the contrary, another fast simulation method, dynamic self-consistent field theory, does not include hydrodynamic effects that may influence the dynamics of structure evolution in the system.

DPD simulation of a CG model of the lipid vesicle is used here to elucidate the generic principles of the cellular membrane damage induced by the shock waves.

2. Model and Methods

The DPD approach, which is a mesoscale technique for the complex fluids, allows simulation of correct hydrodynamic behavior. A DPD system is composed of CG soft particles, each representing clusters of molecules rather than individual atoms, moving continuously in space and discreetly in time according to Newton's equations of motion. In a DPD, particles interact with each other via a pair-wise, two-body, short-ranged force, **F,** that is written as the sum of a conservative force, $\mathbf{F}^C$, dissipative force, $\mathbf{F}^D$, and random force, $\mathbf{F}^R$:

$$\mathbf{F}_i = \sum_{j \neq i} \mathbf{F}_{ij}^C + \sum_{j \neq i} \mathbf{F}_{ij}^D + \sum_{j \neq i} \mathbf{F}_{ij}^R \qquad (1)$$

In this report, $\mathbf{F}^C$ includes a soft repulsion force, $\mathbf{F}^{Cr}$, acting between two particles and a harmonic force, $\mathbf{F}^H$, acting between adjacent particles in a polymer chain.

$\mathbf{F}^C$ forces are derived from interaction potentials described in the following. The remaining two forces, $\mathbf{F}^D$ and $\mathbf{F}^R$, provide the DPD thermostat. The dissipative force modifies the kinetic energy of the particles and is balanced by the random force according to the fluctuation-dissipation theorem. A detailed description of the DPD thermostat can found elsewhere (*7–10*).

DPD-reduced units are adopted for the convenient expression of parameters: length in r_c, energy in k_BT/r_c, mass in particle mass m, and time in $\tau = r_c\sqrt{m/k_BT}$. Standard values in DPD units of $m = k_BT = 1$ and overall particle density $\rho_{DPD} = 3$ were chosen.

The systems considered here are built up from three bead species: lipid head (H), lipid tail (T), and water beads (W). The model lipids have a headgroup consisting of three H beads and two hydrophobic tails, each of which is made up from four T beads (figure 2) and corresponds to a CG model dimyristoyl-phosphatidylcholine (DMPC) of $H_3(C_4)_2$ architecture. Each chain-bead C represents 3.5 CH_2 groups of the level of coarse-graining $N_m = 3.5$. This CG model was used by Grafmüller et al. (*11*).

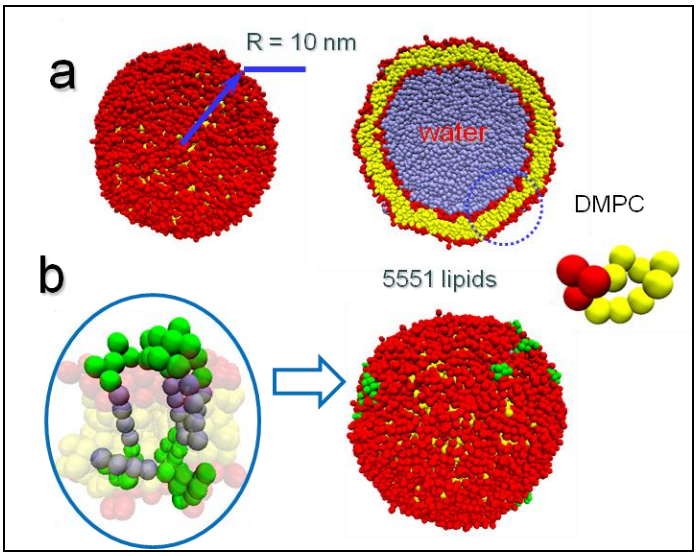

Figure 2. Snapshot of the lipid vesicle (liposome): (a) the liposome is composed from 5551 lipids, and (b) a generic membrane protein is inserted in the membrane. H, T, and W particles are colored red, yellow, and blue, respectively. The generic rod and coil chains are colored cyan and green, respectively.

The pair interaction between topologically nonconnected particles is described by a weakly repulsive potential:

$$U_{DPD}(r) = \frac{a_{DPD}}{2}\left(1 - \frac{r}{r_c}\right)^2 \qquad (2)$$

where a_{DPD} is the maximum repulsion and $r_c = 1$ is the cutoff radius. a_{DPD} differ for different bead species and their values are taken from Grafmüller et al. (*11*).

Table 1. Interaction parameters a_{ijDPD} between pairs of beads. *i* and *j* could belong to head (H), tail (T), or water (W) beads, respectively.

Bead Type	**H**	**T**	**W**
H	30	35	30
T	35	10	75
W	30	75	25

In general, the simulation parameters are chosen to match the mesoscopic behavior of the system.

Topologically connected beads in lipids interact according to the harmonic potential, U_{harm}:

$$U_{harm}(r) = \frac{k}{2}(r - r_0)^2 \qquad (3)$$

where k is the harmonic constant and r_0 is the equilibrium bond distance; the values of $k = 225$ and $r_0 = 0.85$ are used.

In addition, the hydrocarbon chains (tails) are stiffened by a bending potential for two consecutive bonds of the form

$$U_{bend}(r) = k_\theta(1 - \cos\theta) \tag{4}$$

where the potential parameters are $k_\theta = 2$ and $\theta = 180$.

Initial configurations were generated by randomly placing water particles into the simulation box. The vesicle structure was preassembled from 5551 lipids, putting the head groups in the inner and outer parts of the spherical membrane. The final configurations were obtained by the initial equilibration of hydrophobic tails by freezing of the head beads and subsequent short simulation of fully mobile lipids (figure 2a). The vesicle also contains 10 generic membrane proteins modeled by the rod-coil chains (figure 2b). The beads that made up the rigid part are hydrophobic, and their stiffness is controlled by a harmonic angular potential, $U_a(r) = \frac{k_\varphi}{2}(\varphi - \varphi_0)^2$, where $\varphi_0 = 180$ and $k_\varphi = 50$. The hydrophilic beads belong to the flexible part of the protein.

In this study, all of the equilibration stages were performed with $T = 1.0$. The time step was $\Delta t_{DPD} = 0.01$.

Shock waves were initiated with a momentum reflecting mirror, which is a standard method for generating shock waves in computer simulation studies of lipid bilayers (*11*, *12*). This method allows for generation of the fast shock waves with a well-defined shock-wave front and good numerical stability. Infinite-mass piston moves in z positive direction and creates shock waves. All particles coming into contact with the piston surface are reflected, and the velocity relative to the moving wall is flipped in z (*2*).

Upon impact, the target material is compressed and the resulting steep density gradient initiates a shock wave. After a short initial time, the piston was stopped while the initiated shock wave continued to travel further along z direction (figure 3). The speed of the piston, v_p, and the final piston position were varied to get different shock wave profile. The pressure was measured as function of time and distance. The liposome was placed far enough in the simulation box to ensure that it is not to be hit by the piston. This method is similar to standard shock wave experiments where a static target material is hit by a fast-moving impactor (*5*).

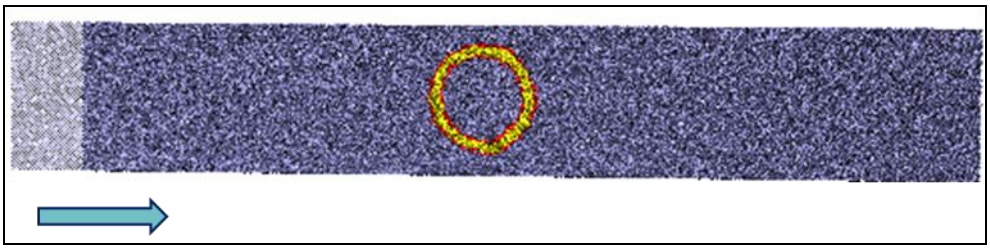

Figure 3. Snapshot of the simulation box after initial compression.

To compare our simulation results with experimental data, it is necessary to define energy, length, and time. The basic length scale, i.e., a physical size of interaction radius, $r_c = 0.69$ nm, is computed from $r_c = \sqrt[3]{\rho_{DPD} N_m v_w}$ nm, where v_m is the volume of one water molecule (*10, 11*). The coupling of the time scales was determined from a ‘‘speed of sound’’ in the DPD fluid, c_{DPD}, which was found to be in a range of 3.818 to 4.298 DPD units (*13*). Having c_{water} = 1497 m/s, the time scale was found to be equal to $\tau = \frac{r_c c_{water}}{c_{DPD}} = 0.25$ ms. The same technique is used for mapping pressure in this simulation to the physical units, where the equilibrium pressure of 22.75 in DPD units was found to be approximately equal to an atmospheric pressure of 14.7 psi.

To determine the speed of the shock wave, the *z* location of the shock wave front was identified as a function of simulation time. The position of the liposome was monitored during the simulation, and pressure impulse and profile were computed.

Since study of the time evolution of the shocked vesicle requires a large box along the direction of the shock impulse, L_z, to allow the shock front to travel for a long period of time, the simulation box is relatively large—35 × 35 ×25 nm—and the liposome is 20 nm in diameter. The simulation box contains approximately 2,500,000 particles.

All simulations were executed using LAMMPS software from Sandia National Laboratories (*14, 15*).

3. Results and Discussion

3.1 Simulation of the Blast Waves with Low Peak Pressure

Figure 4 shows an example of pressure profiles during the simulation at various distances from the initiation of the shock wave that mimics the distance of the center of the explosion. The point of the shock wave initiation is defined here as the center of the explosion. As expected, the peak overpressure decreases with distance from the center of the explosion (see figure 4a). These curves closely mimic the supersonic shock wave produced by high explosives passing through the head. This wave causes almost instantaneous overpressure, followed by a longer wave of

underpressure, and a second wave of overpressure (*1*). The similar shock wave was experimentally obtained by a pneumatic device that delivers shock waves (*5*).

The curves shown in figure 4 correspond to the shock wave with the Mach number $M = 1.29$, where the Mach number is a dimensionless quantity representing the ratio of speed of the shock wave in a fluid and the local speed of sound. The magenta curve represents the change in pressure at the location of the liposome, which was placed at 117.4 nm from the center of the explosion and did not move significantly (figure 4a). The pressure profiles that corresponds to the same system at the time of the peak overpressure at the vesicle location (t = 6.75 ms) is shown in figure 4b.

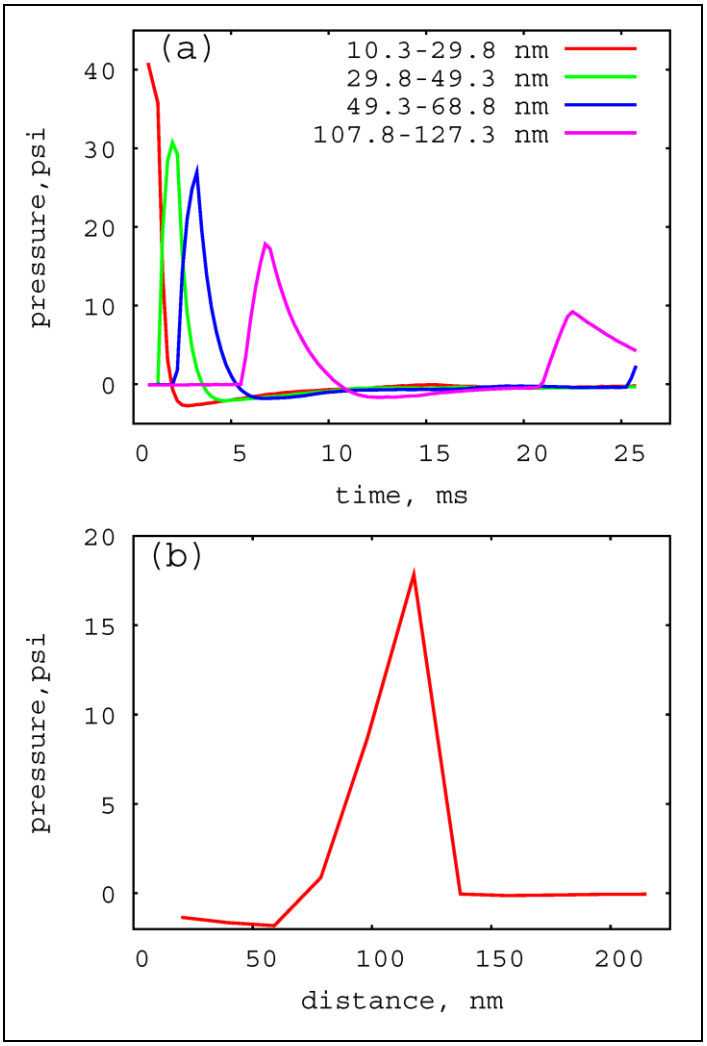

Figure 4. (a) The supersonic shock blast wave at the various distances from its launch. The liposome location corresponds to the magenta curve. The second peak in blue and magenta curves represents the second positive phase due to reflection. The Mach number is 1.29. (b) The pressure profile at time = 6.75 ms after the explosion at the liposome location.

To get different pressure profiles for mild shock, the piston speed v_p was varied, keeping the compression of the box constant. Values of v_p were equal to 7485 m/s, 14,970 m/s, and 22,455 m/s, respectively. This technique produces the blast waves with the Mach numbers of 1.29, 1.43, 1.48, respectively, and overpressure peaks equal to 17.8, 24.6, and 31.4 psi, respectively. The overpressure peaks were measured at approximately 117.6 nm (at the location of the liposome).

The results are reported in figure 5. The liposome is moved in the positive *z* direction during the simulation, as the shock wave hits it, and then the liposome flows in the negative *z* direction as the reflective wave reaches its location (the second positive phase). The movement of liposome in the lateral direction to the shock wave is found to be negligible (less than 1%). With the increase of v_p, the reflective wave hits the liposome before the pressure reaches the ambient value.

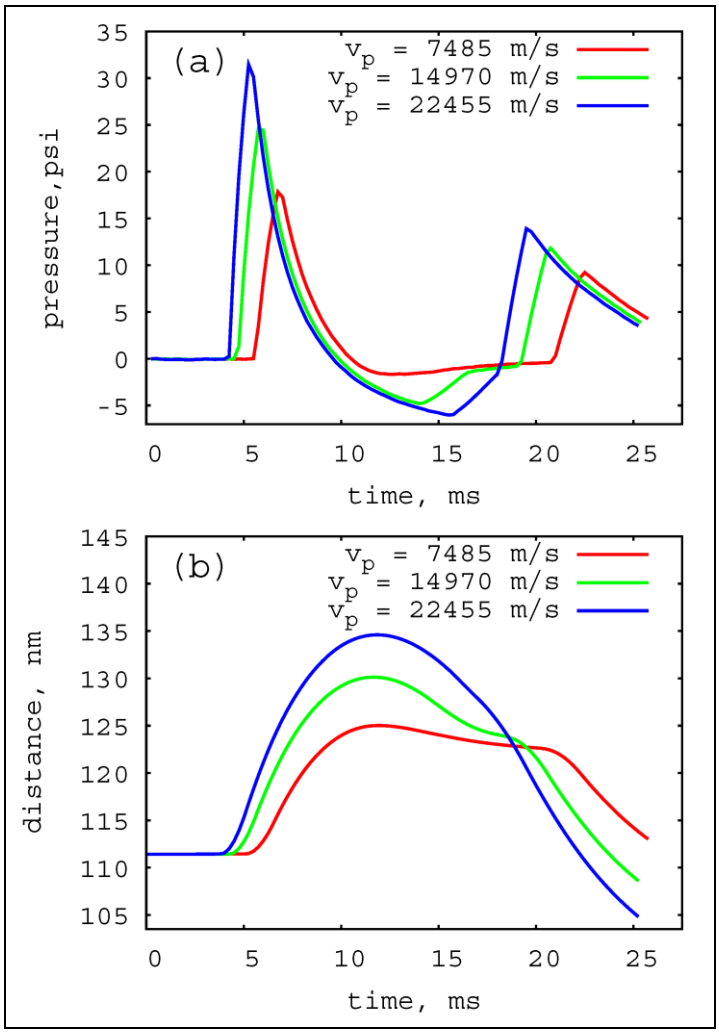

Figure 5. (a) Shock wave at the location of the liposome for the various piston speeds v_p. (b) Movement of the center of mass of the liposome in *z* direction.

To characterize the deviation from an equilibrium vesicle structure, the diagonal principle moments of the gyration tensor, λ_{xx}^2, λ_{yy}^2, and λ_{zz}^2, were computed, which are given by

$$\lambda_{dd}^2 = \frac{1}{N}\sum_{i=0}^{N}\left(r_{id} - r_{com}\right)\left(r_{id} - r_{com}\right) \tag{5}$$

where r_{com} represents the coordinates of the liposome center of mass and N is number of beads in the liposome. Figure 6 shows the change in λ_{dd}^2 in time. The results of this study suggest that changes in λ_{xx}^2 and λ_{yy}^2 are insignificant compared with the change in λ_{zz}^2. The liposome is compressed during the positive phase, then it is extended at the negative phase and the process repeats with lower values of compression/extension for the reflective wave. Notably, an extent of the liposome compression does not strongly depend on the pressure pulse compared with an extent of liposome extension (figure 6b). This finding suggests that the liposome extension is very sensitive to the change in the negative pressure phase, which can consequently lead to more structural damage of the cell membranes.

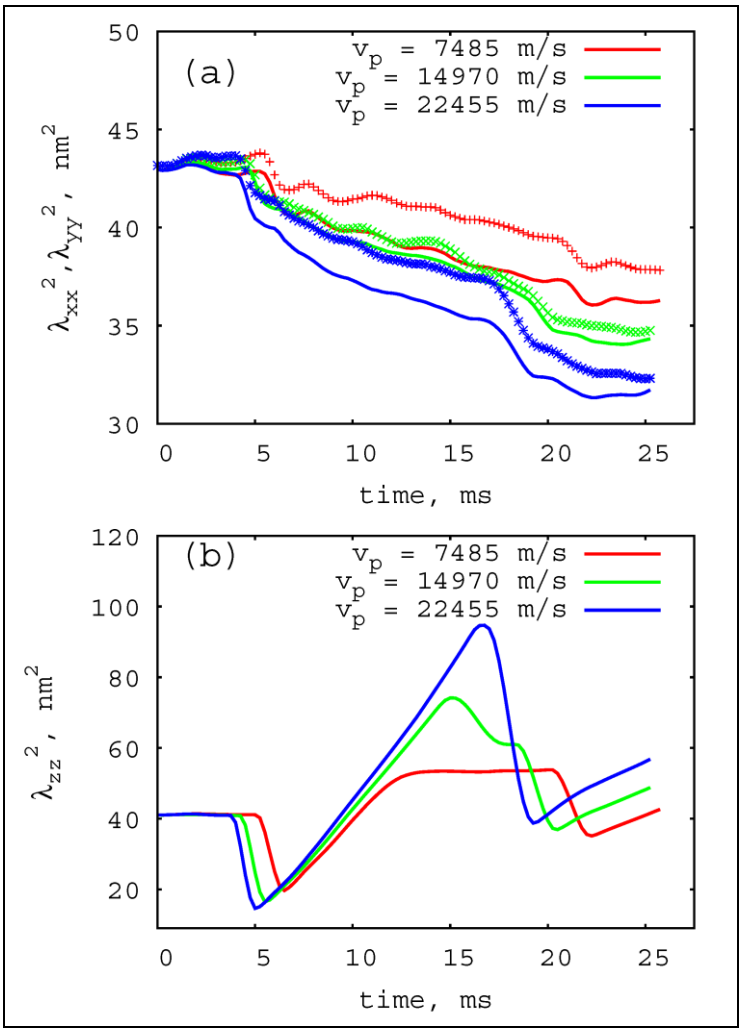

Figure 6. Change in the diagonal principle moments of the gyration tensor (a) λ_{xx}^2, λ_{yy}^2, and (b) λ_{zz}^2 during the simulation.

Figure 7a shows vesicle structures at the peak overpressure, which corresponds to the most compressed liposome configurations. At this range of overpressure (17.8–31.4 psi), the liposome membrane does not sustain any significant damage; even the liposome is compressed. Figure 7b demonstrates substantial extension of the vesicle at the considering negative pressure range (1.7–6.0 psi).

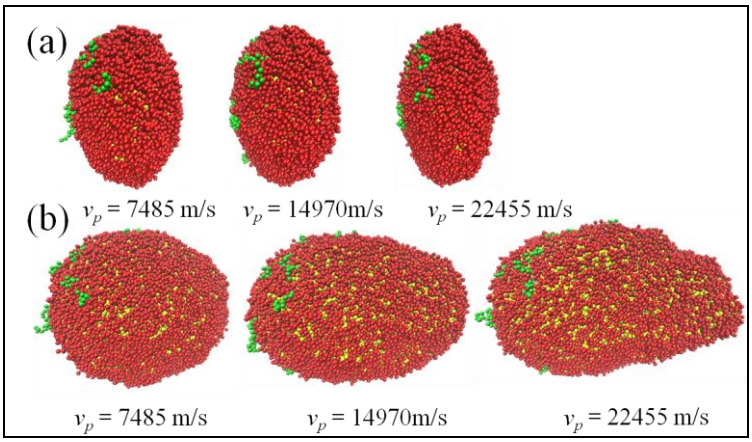

Figure 7. Snapshot from the liposome simulation at the various piston speeds: (a) compressed structures and (b) extended structures. For visual clarity, water particles are not shown. H and T particles are colored red and yellow, respectively. The generic rod and coil chains are colored cyan and green, respectively.

Even visually intact, the liposome membrane starts to have perforation in its hydrophobic (inner) layer at negative pressure, approximately −4.8 psi. Figure 8 shows a small hole in hydrophobic part of the bilayer. The results imply that the cellular membrane permeability is altered even for the small negative pressure, and consequently sodium, potassium, and calcium ion influx may change. This finding suggests that the cellular damage leading to the TBI may take place because of the relatively low negative pressure.

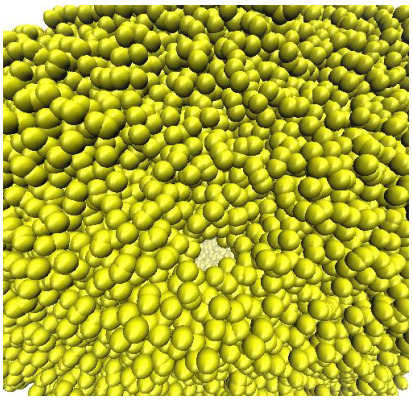

Figure 8. Part of the liposome hydrophobic layer with a hole. For visual clarity, only hydrophobic particles are shown.

3.2 Simulation of the Blast Waves with High Peak Pressure

In order to get higher overpressure, two simulations were performed with the piston speed v_p equal to 7485 m/s and 14,970 m/s, respectively. In these simulations, the piston was allowed to move longer, and therefore both positive and negative pressure phase values are greater than the

previous simulation of the mild shock (figures 5a and 9a). The Mach numbers of these waves are close: 1.85 and 1.89, which correspond to v_p equal to 7485 m/s and 14,970 m/s, respectively. Since the shock waves move faster in this series of simulations, the reflection wave reaches the liposome earlier than in the previous simulations. The durations of the positive and negative phases are close to the previous simulation (figures 5a and 9a).

The liposome flows in the positive z direction at the greater distance compared with the mild shock (figures 5b and 9b).

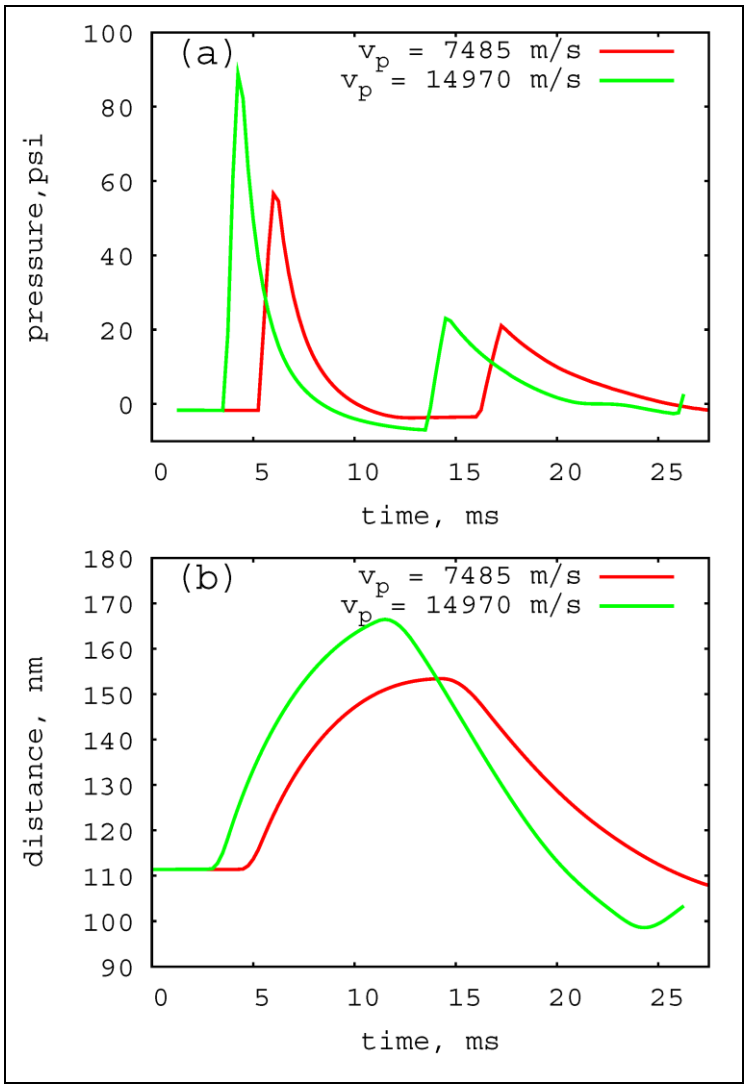

Figure 9. (a) Shock wave at the location of the liposome for the various piston speeds v_p. (b) Movement of the center of mass of the liposome in z direction.

Change in the diagonal principle moments of the gyration, λ_{xx}^2 and λ_{yy}^2, is slightly more pronounced than the mild shock. λ_{zz}^2 decreases significantly more for this series due to higher peak overpressure (figures 6b and 10b). Interestingly, that the liposome undergoes less extension

in the *z* direction for the simulation with v_p = 14,970 m/s than the liposome in the simulation of v_p = 7485 m/s (figure 10b). This effect caused by the reflective wave that reaches the liposome before the vesicle was fully stretched.

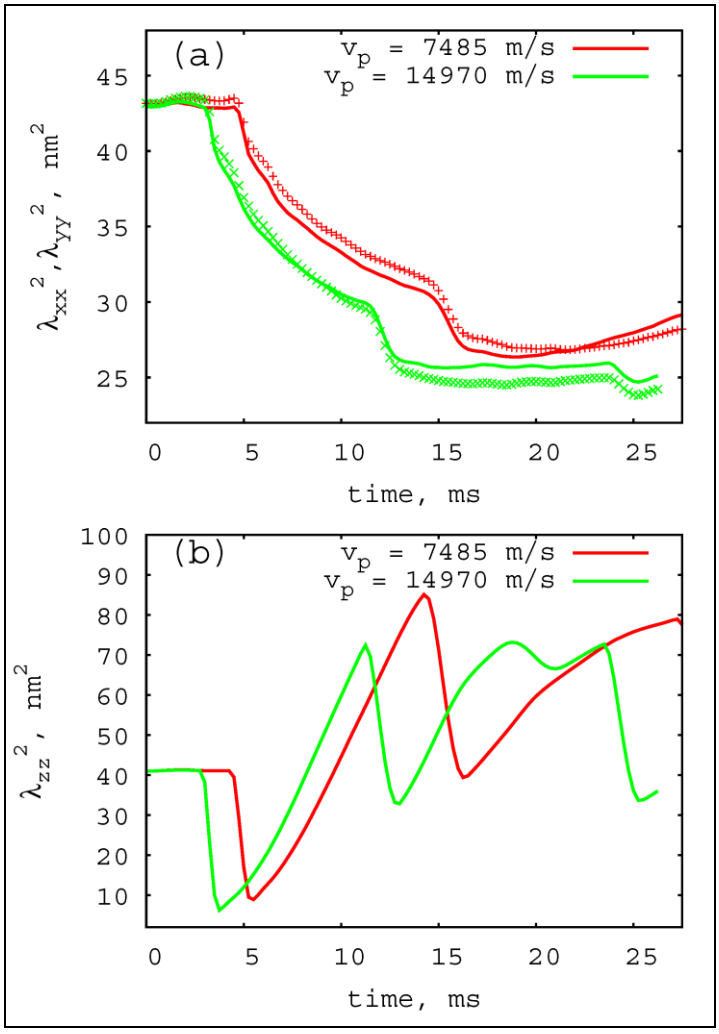

Figure 10. Change in the diagonal principle moments of the gyration tensor (a) λ_{xx}^2, λ_{yy}^2, and (b) λ_{zz}^2 during the simulation.

The simulation results show that perforation in the hydrophobic (inner) layer of the liposome membrane begins at the positive pressure. Note that approximately 90 psi of the overpressure causes the significant membrane perforation. Figure 11 shows a large hole in hydrophobic layer of the compressed vesicle.

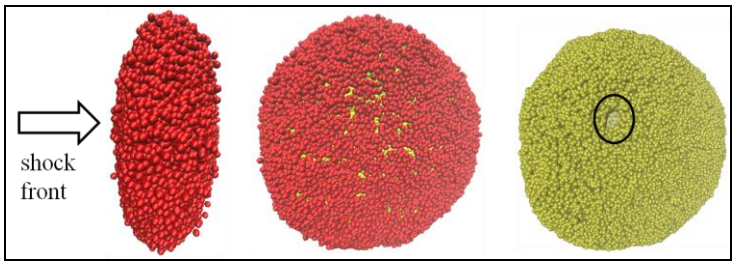

Figure 11. Compressed liposome. H and T particles are colored red and yellow, respectively. For visual clarity, water and protein particles are not shown. The circle shows a location of a hole in the hydrophobic layer.

4. Conclusion

The simulation findings suggest that the cellular membrane permeability is altered even for a relatively mild shock wave ($M < 1.5$) in the negative pressure phase. It was found that the small negative pressure, approximately −5 psi, may lead to the cellular damage by changing the ion influx. The faster-moving shock waves ($M \approx 1.9$), which gave higher overpressure peaks, already cause the cellular damage in the positive pressure phase if peak overpressure is greater than 60 psi. In future work, we will extend our approach to characterize the change of specific permeability of the cellular membranes induced by the shock blast waves. Since the real brain cell membranes are inhomogeneous structures that include multiple lipids, cholesterol, and numerous proteins, we will develop a model of the cellular membrane with a higher level of accuracy. The results of this improved model of the cellular membrane will be incorporated into the multilevel modeling of electrochemical connectivity of large-scale brain networks.

5. References

1. Duncan, C. C.; Summers, A. C.; Perla, E. J.; Coburn, K. L.; Mirsky, A. F. Evaluation of Traumatic Brain Injury: Brain Potentials in Diagnosis, Function, and Prognosis. *Int. J. Psychophysiol*. **2011**, *82*, 24–40.

2. Ganzenmüller, G. C.; Hiermaier, S.; Steinhauser, M. O. Shock-Wave Induced Damage in Lipid Bilayers: A Dissipative Particle Dynamics Simulation Study. *Soft Matter* **2011**, *7*, 4307–4317.

3. Ganpule, G. S. Mechanics of Blast Loading on Post-Mortem Human and Surrogate Heads in the Study of Traumatic Brain Injury (TBI) Using Experimental and Computational Approaches. Ph.D. dissertation, University of Nebraska-Lincoln, 2013.

4. Bowen, I. G.; Fletcher, E. R.; Richmond, D. R.; Hirsch, F. G.; White, C. S. Biophysical Mechanisms and Scaling Procedures Applicable in Assessing Responses of Thorax Energized by Air-Blast Overpressures or by Nonpenetrating Missles. *Annals of the New York Academy of Sciences* **1968,** *152*, 122–146.

5. Ravin, R.; Blank, P. S.; Steinkamp, A.; Rappaport, S. M.; Ravin, N.; Bezrukov, L.; Guerrero-Cazares, H.; Quinones-Hinojosa, A.; Bezrukov, S. M.; Zimmerberg, J. Shear Forces During Blast, Not Abrupt Changes in Pressure Alone, Generate Calcium Activity in Human Brain Cells. *Plos One* **2012**, *7*, e39421.

6. Marrink, S. J.; de Vries, A. H.; Tieleman, D. P. Lipids on the Move: Simulations of Membrane Pores, Domains, Stalks, and Curves. *Biochimica et Biophysica Acta* **2009**, *1788*, 149–168.

7. Hoogerbrugge, P. J.; Koelman, J. M. V. A. Simulating Microscopic Hydrodynamic Phenomena With Dissipative Particle Dynamics. *Europhys. Lett.* **1992**, *19*, 155.

8. Koelman, J. M. V. A.; Hoogerbrugge, P. J. Dynamic Simulation of Hard Sphere Suspensions Under Steady Shear. *Europhys. Lett.* **1993**, *21*, 363.

9. Espaňnol, P.; Warren, P. B. Statistical-Mechanics of Dissipative Particle Dynamics. *Europhys. Lett.* **1995**, *30*, 191.

10. Groot, R. D.; Rabone, K. L. Mesoscopic Simulation of Cell Membrane Damage, Morphology Change, and Rupture by Nonionic Surfactants. *Biophys. J.* **2001**, *81*, 725.

11. Grafmüller, A.; Shillcock, J.; Lipowsky, R. The Fusion of Membranes and Vesicles: Pathway and Energy Barriers From Dissipative Particle Dynamics. *Biophys. J.* **2009**, *96*, 2658–2675.

12. Koshiyama, K.; Kodama, T.; Yano, T.; Fujikawa, S. Structural Change in Lipid Bilayers and Water Penetration Induced by Shock Waves: Molecular Dynamics Simulations. *Biophys. J.* **2006**, *91*, 2198–2205.

13. Soares, J. S.; Gao, C.; Alemu, J.; Slepian, M.; Bluestein, D. Simulation of Platelets Suspension Flowing Through a Stenosis Model Using a Dissipative Particle Dynamics Approach. *Ann. Biomed. Eng*. **2013**, *41*, 2318.

14. Plimpton, S. Fast Parallel Algorithms for Short-Range Molecular Dynamics. *J. Comp Phys.* **1995**, *117*, 1.

15. Sandia Laboratories Home Page. *LAMMPS Molecular Dynamics Simulator*. http://lammps.sandia.gov (accessed on 10/30/2013).

NO. OF COPIES	ORGANIZATION
1 (PDF)	DEFENSE TECHNICAL INFORMATION CTR DTIC OCA
1 (PDF)	DIRECTOR US ARMY RESEARCH LAB IMAL HRA
1 (PDF)	DIRECTOR US ARMY RESEARCH LAB RDRL CIO LL
1 (PDF)	GOVT PRINTG OFC A MALHOTRA
1 (PDF)	DIR USARL RDRL WMM G Y SLIOZBERG

INTENTIONALLY LEFT BLANK.